Carbohydrate Polymers 356 (2025) 123412

Contents lists available at ScienceDirect

Carbohydrate Polymers

journal homepage: www.elsevier.com/locate/carbpol

Advanced cyclodextrin-based multiloaded hydrogels for targeted drug delivery in the fight against vaginal fungal infections

Elisabetta Grazia Tomarchio [a,b], Chiara Zagni [a,*], Sandro Dattilo [c], Libera Vitiello [c], Virginia Fuochi [b], Salvatore Furnari [b], Pio Maria Furneri [b], Giuseppe Granata [d], Sabrina Carola Carroccio [c], Antonio Rescifina [a]

[a] Department of Drug and Health Sciences, University of Catania, V.le A. Doria 6, 95125 Catania, Italy
[b] Department of Biomedical and Biotechnological Sciences, University of Catania, Via Santa Sofia 97, 95123 Catania, Italy
[c] Institute for Polymers, Composites, and Biomaterials CNR-IPCB, Via Paolo Gaifami 18, 95126 Catania, Italy
[d] Institute of Biomolecular Chemistry CNR-ICB, Via Paolo Gaifami 18, 95126 Catania, Italy

ARTICLE INFO

Keywords:
Hydrogel
Curcumin
Drug delivery
Cyclodextrin
Clotrimazole

ABSTRACT

Vulvovaginal candidiasis (VVC) affects a significant proportion of women during reproductive years, with recurrent infections posing a considerable therapeutic challenge. Conventional treatments, such as clotrimazole (Clo) administration, often require frequent application due to low aqueous solubility and rapid clearance.

To address these issues, a novel hydrogel-based drug delivery system (DDS) was developed, combining β-cyclodextrins (β-CD) for Clo encapsulation and halloysite nanotubes (HNT) for curcumin (Cur) delivery. A novel hydrogel-based drug delivery system (DDS) was developed to address these limitations to enhance drug solubility, retention, and localized release. β-CD enhanced Clo's solubility and prolonged antifungal effects, while HNT ensured sustained Cur release for up to 5 days, offering anti-inflammatory, antioxidant, and antimicrobial benefits. The hydrogel matrix improved drug retention and stability, with HNT reinforcing its mechanical properties for durability under moderate strain. Microbiological tests demonstrated potent antifungal activity, with inhibition zones of 39.2 ± 0.2 mm, 39.1 ± 0.2 mm, and 42.1 ± 0.2 mm against *C. krusei*, *C. albicans* 10231, and *C. parapsilosis* 22019, respectively. Drug release studies revealed a rapid burst release of Clo within the first 30 min, followed by prolonged Cur release. This dual-action hydrogel targets fungal infections, oxidative stress, and inflammation, providing enhanced therapeutic outcomes and improved patient adherence.

1. Introduction

Vulvovaginal candidiasis (VVC) affects up to 75 % of women during reproductive years, with 40 % experiencing recurrence (Mahant et al., 2023). First-line treatments include vaginal clotrimazole (Clo) and miconazole, with oral antimycotics reserved for severe or recurrent cases (Reef et al., 1993). The systemic bioavailability of vaginal antimycotic drugs is generally low, meaning that only minimal amounts of the drug enter the bloodstream, reducing systemic side effects. To improve therapeutic outcomes, researchers focus on creating efficient drug delivery systems (DDS) that provide localized and sustained drug release (Carbone et al., 2020; Ezike et al., 2023a; Furneri et al., 2017). These systems optimize localized treatments by taking advantage of vaginal administration, which offers a large absorption surface and bypasses first-pass metabolism, all while enhancing patient comfort and compliance.

Polymeric materials with macroporous structures, such as hydrogel or cryogel, are ideal candidates as drug delivery systems offer a promising approach for localized treatment of infections, particularly when designed with materials that ensure controlled release and low toxicity (Dreiss, 2020; Raina et al., 2022; Varaprasad et al., 2017; Zagni et al., 2024). The limitation of hydrogels is their hydrophilicity, which determines the lack of adsorption of hydrophobic species. A strategy to overcome this problem is to design host-guest supramolecular systems with hydrophobic cavities, such as polymeric nanocarriers based on cyclodextrins (Peng et al., 2017). Clo, a topical broad-spectrum antifungal agent, is a fungistatic agent that alters the permeability of the cell membrane, leading to the destruction of fungal cells (Crowley & Gallagher, 2014). This drug is highly lipophilic (logP 4.1) with low aqueous solubility (0.49 mg/L) and requires frequent applications to sustain

* Corresponding author.
E-mail address: chiara.zagni@unict.it (C. Zagni).

https://doi.org/10.1016/j.carbpol.2025.123412
Received 24 December 2024; Received in revised form 29 January 2025; Accepted 15 February 2025
Available online 16 February 2025

therapeutic levels (Pedersen, 1993). For this reason, researchers reported the complexation of Clo with β-cyclodextrin (β-CD) to increase its solubility (Mohammed et al., 2016). In addition, incorporating Clo into advanced drug delivery systems (DDS) not only improves its solubility but also ensures controlled and localized release, reducing application frequency and enhancing overall treatment efficacy. Various DDS containing Clo have already been reported. Among these, mucoadhesive thermosensitive gels combining poloxamers and polycarbophils have been shown to boost and sustain Clo's antifungal efficiency compared to conventional formulations (Ezike et al., 2023b). Additionally, poly (lactic-*co*-glycolic) acid nanoparticles surface-modified with chitosan demonstrated enhanced mucoadhesive properties and improved delivery for vaginal applications, highlighting the potential of these systems in optimizing clotrimazole therapy (Martínez-Pérez et al., 2018).

However, while these systems are highly effective in drug release, they often suffer from stability issues and mechanical weaknesses. Specifically, many of these systems do not exhibit high mechanical strength, which can hinder their performance in the long term, particularly in vaginal applications where structural integrity is crucial for sustained drug delivery. To address limitations in mechanical properties often observed in these DDS, the incorporation of HNT represents a strategic solution. Beyond serving as structural reinforcements that enhance the mechanical strength and durability of the system, HNT, a naturally occurring, biocompatible clay with a high surface area and a hollow lumen, also offer unique advantages in molecular encapsulation. Their ability to load and release a wide variety of drugs makes them ideal for controlled and sustained delivery, particularly in vaginal drug delivery systems (Li et al., 2016; Vergaro et al., 2010). Furthermore, HNT are safe with no significant toxicity to biological cells, making them suitable for biomedical applications (Zagni, Scamporrino, Riccobene, et al., 2023). However, in their native powdered form, HNT face challenges in handling due to dispersion issues and lack of structural integrity. To address these concerns, embedding HNT within a polymer matrix, such as a hydrogel, creates a stable and easily applicable system (Witika et al., 2021).

Candidiasis, particularly in recurrent or resistant cases, involves fungal infections, inflammation, oxidative stress, and disruption of the host's microbiome balance (Cheng et al., 2024; d'Enfert et al., 2020; Fuochi et al., 2017). These additional factors necessitate a more comprehensive therapeutic approach beyond antifungal treatment. Incorporating bioactive compounds with complementary properties, such as curcumin (Cur), offers a promising strategy to tackle these challenges. Cur, a natural polyphenol derived from *Curcuma longa*, has demonstrated potent anti-inflammatory, antioxidant, and antimicrobial activities, making it an ideal adjunct to Clo in treating vaginal infections (Lin & Lee, 2006). By encapsulating Cur within HNT, sustained and localized release at the site of infection is achieved, thereby improving therapeutic efficacy and addressing the oxidative stress and inflammation commonly associated with candidiasis (Witika et al., 2021). This approach enhances therapeutic efficacy by promoting healing and restoring microbiome balance, offering a comprehensive solution for recurrent or resistant infections. The intrinsic properties of HNT ensure prolonged residence time within the vaginal environment, allowing for the controlled release of Cur and enhancing overall treatment outcomes. Addressing both the infection and the broader pathological environment provides a more effective and holistic treatment for candidiasis (Andrade et al., 2019; Chen et al., 2022).

Addressing the infection and its broader pathological environment becomes possible, providing a more effective and holistic treatment for candidiasis, a natural compound with a wide range of therapeutic properties.

The combination of these two strategies, β-CD for Clo and HNT for Cur, offers a dual therapeutic approach that could be particularly valuable for the treatment of vaginal mycotic infections, potentially providing a more efficient and sustained treatment strategy. Such infections require antifungal activity, which is effectively provided by Clo, and benefit from anti-inflammatory and antioxidant actions to mitigate inflammation and oxidative stress in the affected tissues. Cur-loaded HNT could fulfill this role, complementing the antifungal effects of Clo by addressing secondary inflammation and enhancing tissue recovery. Cur has demonstrated significant antifungal activity by disrupting fungal cell membranes through multiple mechanisms, including inhibiting hydrogen ion efflux, reduced ergosterol levels, and decreased proteinase secretion (Lee & Lee, 2014). Studies have shown its efficacy in treating oral candidiasis and improving oral mucositis in clinical and animal models (Karaman et al., 2011). Evidence suggests that curcumin enhances azole efficacy against resistant fungal strains. Notably, curcumin at 11 μM concentration has been shown to restore fluconazole sensitivity in *C. albicans* by inhibiting an efflux pump, likely belonging to the major facilitator superfamily transporters. This finding highlights curcumin's dual role as a direct antifungal agent and an effective adjuvant in overcoming azole resistance (Garcia-Gomes et al., 2012).

To this end, a new system based on natural and biocompatible compounds has been proposed to deliver a broad-spectrum therapeutic approach. This system takes advantage of β-CD ability to encapsulate small molecules, serving as an effective carrier for Clo, a poorly water-soluble yet widely used azolic antimycotic agent with a well-established antifungal efficacy against vaginal infections. Concurrently, incorporating HNT provides a robust and stable platform for the sustained release of Cur, a natural compound with potent antioxidant, anti-inflammatory, and moderate antifungal and antimicrobial effects.

This paper investigates the synthesis and characterization of a novel hydrogel composed of a cyclodextrin derivative-Clo complex integrated with HNT for vaginal drug delivery, focusing on its capability for sustained and controlled drug release. The study further examines the release profiles of Clo and Cur and evaluates the mechanical properties of the hydrogel.

2. Experimental

2.1. Materials

Clo, β-CD, Cur, acryloyl chloride, sodium hydride in mineral oil (60 %), acetone, dimethyl-formamide anhydrous (DMF), DMSO-d_6, 2-hydroxyethyl methacrylate (HEMA), *N*,*N*′-methylene-bisacrylamide (MBAA), ammonium persulfate (APS), tetramethyl-ethylene-diamine (TEMED), ethanol and halloysite nanotubes were purchased from Merk. A Milli-Q water purification system was used to produce deionized water. ^{1}H NMR spectrum was recorded at 300 K on Varian UNITY Inova using DMSO-d_6 as solvent.

2.2. Chemistry

2.2.1. Synthesis of β-CD-acrylate monomers (CDA)

β-CD-acrylate monomers were synthesized according to the procedure reported in the literature (Zagni, Coco, Mecca, et al., 2023). Briefly, β-CD (1 g, 0.8811 mmol) was dissolved in DMF (10 mL) and cooled to 0 °C, under nitrogen. NaH (84.55 mg, 3.5244 mmol, 4 eq) was introduced, and the reaction mixture was stirred for 30 min. Subsequently, acryloyl chloride (285.54 μL, 3.5244 mmol, 4 eq) was added dropwise, and the mixture was stirred for 24 h at room temperature. Afterwards, the solution was concentrated under vacuum. Cold acetone was added, and the white solid formed was collected by filtration and dried in an oven for 24 h. Yield 85 %. ^{1}H NMR (500 MHz, DMSO-d_6): $\delta = 6.43–6.03$ (m, 4H), 5.99–5.76 (m, 2H), 5.72–5.34 (m, 12H), 4.88–4.70 (m, 6H), 4.66–4.33 (m, 8H), 3.85–3.71 (m, 7H), 3.69–3.56 (m, 16H), 3.31–3.24 (m, 6H).

2.2.2. Synthesis of β-CD acrylate – clotrimazole inclusion complex (CDA-Clo)

Equimolar amount of β-CD acrylate and Clo, as dry powders, were co-grinded in a mortar without solvent for 20 min. (Jablan et al., 2013) The

obtained mixture was dried under vacuum to reduce the air moisture. The obtained product was characterized by the TGA, DSC, and FT-IR analysis described in the following section.

2.2.3. General synthesis of drug-loaded HNT

HNT was loaded with the drug using a general solution absorption method. In detail, 60 mg of HNT was dispersed into 1 mL ethanolic solution of Cur (20 mg/mL) and sonicated for 20 min to promote drug uptake into nanotubes. Then, after a rest period of 10 min, the mixture was left under vacuum for 20 min, promoting air bubble removal from nanotubes. The procedure was repeated three times. The crude drug-loaded HNT was separated by centrifugation and washed three times with ethanol to remove any unabsorbed drug from the surface. Finally, the product was dried at 40 °C under vacuum to obtain drug-loaded HNT.

2.2.4. Synthesis of CDA-Clo based hydrogel (H_CDA-Clo)

Hydrogel containing CDA-Clo complex was synthesized by a free radical polymerization process at room temperature. Specifically, functionalized monomers CDA-Clo and HEMA, used as co-monomer, were dissolved in water at a weight ratio of 1:1. The cross-linking agent MBAA was added at a monomers/crosslinker molar ratio of 6:1 and mixed until complete dissolution. The amount of water was then corrected to obtain a total content of polymerizable compounds of 10 % *w/v* of the solution. Then, 2 % *v*/v of a water solution of APS at a concentration of 10 % w/v was added, followed by 2 % v/v of a water solution of TEMED at a concentration of 10 % w/v. The mixture was stirred for 1 min, distributed into a multiwell plate, and left to polymerize for 3 h at room temperature. Afterward, samples were washed with water and ethanol and dried under nitrogen flux. Finally, all samples were dried under a vacuum overnight at 40 °C.

2.2.5. Synthesis of CDA-Clo/HNT-Cur hydrogel (H_CDA-Clo/HNT-Cur)

Hydrogel containing CDA-Clo complex and HNT-Cur was synthesized according to the procedure reported for synthesizing H_CDA-Clo by adding 20 % wt of HNT-Cur to the monomers and crosslinker mixture.

Under the same conditions, the reference blank H_CDA/HNT was synthesized using pure CDA and HNT. Furthermore, H_CDA-Clo/HNT and H_CDA/HNT-Cur were also synthesized.

2.3. Characterization

2.3.1. Infrared spectroscopy (FT-IR)

FT-IR analyses were performed in the 4000–550 cm^{-1} spectral range using a PerkinElmer FTIR System 2000 (Waltham, MA, USA), with potassium bromide (KBr) pellet technique.

2.3.2. Thermogravimetric analysis (TGA)

TGA was carried out using a TA Instruments Q500 apparatus under a nitrogen atmosphere (flow rate of 60 mL/min), with a heating rate of 10 °C/min, over a temperature range of 40 °C to 800 °C. The TGA system features a sensitivity of 0.1 μg and a weighing precision of ±0.01 %, with an isothermal temperature accuracy of ±1 °C.

2.3.3. Differential scanning calorimetry (DSC)

DSC measurements of samples were conducted using a TA Instruments Q100 DSC calorimeter (Milan, Italy) equipped with a liquid sub-ambient accessory. Approximately 4 mg of the sample was sealed in an aluminum pan, equilibrated at 75 °C, and subjected to a heating cycle from −25 °C to 400 °C.

2.3.4. Scanning electron microscopy (SEM)

Hydrogel's morphologies were analyzed using SEM. To enhance conductivity, the samples were pre-coated with a thin gold layer (<10 nm). Characterization was performed using a Thermo Phenom ProX desktop SEM (Thermo Fisher Scientific, Waltham, MA, USA).

2.3.5. Swelling measurement

The swelling behavior of hydrogels was assessed by determining their water absorption capacity. The hydrogel samples were dried in an oven at 50 °C until a constant weight was achieved. The dried weight (W_0) of each sample was recorded using an analytical balance with a precision of 0.01 mg.

Subsequently, the dried hydrogel samples were immersed in distilled water at room temperature for 1 h. After swelling, the samples were removed from the water and gently blotted with filter paper to remove surface water without disturbing the swollen structure. The swollen weight (W_s) was then measured using the same analytical balance.

The swelling ratio (SR) was calculated using the following equation:

$$SR = \frac{(W_s - W_0)}{W_0} \quad (1)$$

All experiments were performed in triplicate, and the results are presented as mean values with standard deviation.

2.4. Drug release experiments

The release kinetics of Clo from the hydrogels was evaluated in two different media: a neutral pH environment (PBS buffer-methanol mixture, pH 7.4) and an acidic environment (acetate buffer, pH 4.5).

For the neutral pH condition, a defined quantity of hydrogel containing Clo was placed in a vial containing a 3:1 mixture of PBS buffer (pH 7.4) and methanol. For the acidic condition, the acetate buffer (pH 4.5) was prepared by adjusting a 2 M sodium acetate solution with glacial acetic acid until the desired pH was reached. A defined quantity of the hydrogel was then immersed in the buffer solution.

In both cases, the vials were gently agitated on an orbital shaker at room temperature.

At specific time intervals (0, 5, 10, 15, 30, 40, 60, 80, 120, and 180 min), aliquots of the release medium were collected and analyzed for Clo concentration at 204 nm using UV–Vis spectrophotometry. After each sampling, an equal volume of fresh-release medium was added to maintain sink conditions.

The release kinetics of Cur from the hydrogel was evaluated in a neutral pH environment (PBS buffer-ethanol mixture, pH 7.4) and an acidic environment (acetate buffer, pH 4.5).

For the neutral pH condition, a known amount of hydrogel was incubated in a PBS buffer (pH 7.4)/ethanol solution (50 % *v*/v). For the acidic condition, the acetate buffer (pH 4.5) was prepared as previously described with 15 % Tween 80 and 5 % absolute ethanol to maintain sink conditions. The system was stirred at 50 rpm and maintained at 37 °C ± 2 °C, following the procedure reported in the literature (Nicolau Costa et al., 2021).

In both systems, the vials were gently agitated on an orbital shaker at room temperature. Samples were collected at defined intervals (0, 5, 10, 20, 40, 100, and 180 min; 2, 5, and 8 days). The release medium was analyzed for Cur concentration at 425 nm at each interval using UV–Vis spectrophotometry.

Each experiment was performed in triplicate, and the results are presented as mean values.

2.5. Kinetic model of release

The release behavior of H_CDA-Clo/HNT-Cur hydrogels was analyzed using Prism software to calculate the coefficient of determination (R) and evaluate its fit to various mathematical models commonly applied in drug delivery systems.

The linearized forms of the models, including zero-order kinetics, first-order kinetics, Korsmeyer-Peppas, Higuchi, and Weibull models, were employed to determine the kinetic release parameters. These models are represented in Eqs. (2)–(6) below.

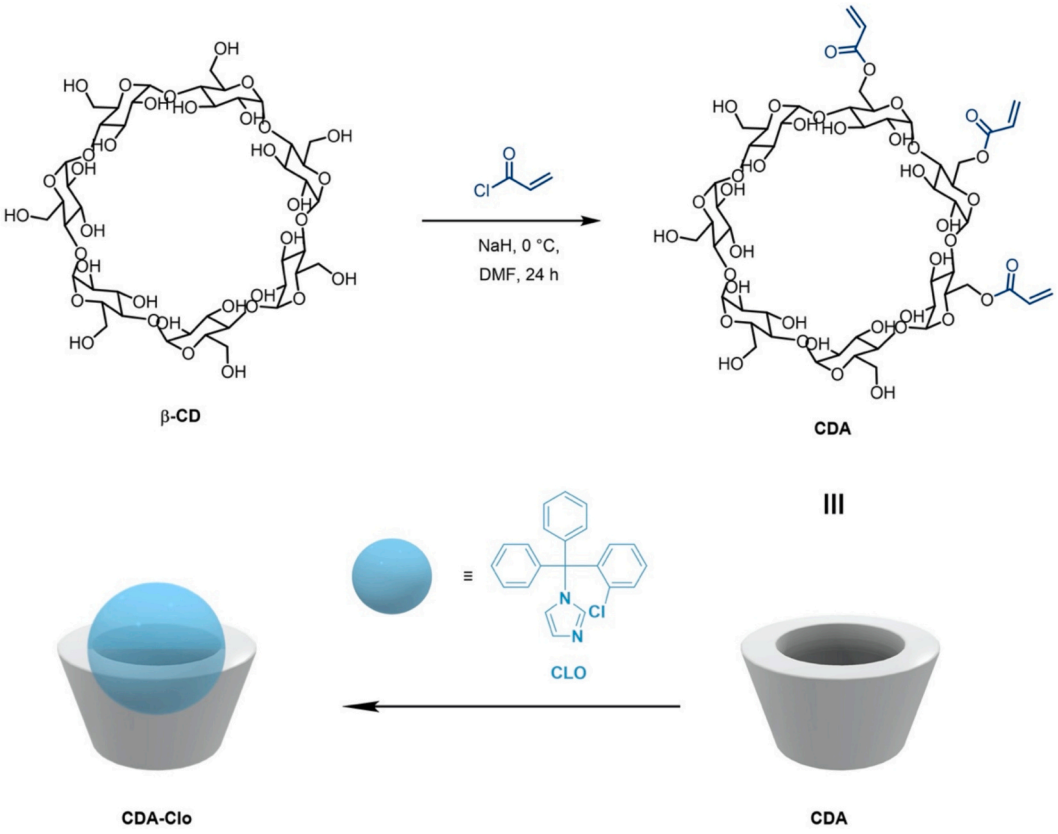

Fig. 1. Schematic representation of the synthesis of CDA-Clo complex.

Zero-order kinetics:

$$M_t/M_\infty = k_0 t \tag{2}$$

This kinetic model describes a constant release rate over time, typically associated with processes such as solid dissolution (Siepmann & Siepmann, 2013).

First-order kinetics:

$$M_t/M_\infty = 1 - e^{-k_1 t} \tag{3}$$

In this case, the drug release is concentration-dependent, meaning it decreases over time as the concentration of the drug reduces (Mulye & Turco, 1995).

Korsmeyer-Peppas (KP) model:

$$M_t/M_\infty = k_3 t^n \tag{4}$$

This equation was developed to describe drug release from polymeric matrix systems (Peppas, 1985).

$$M_t \Big/ M_\infty = k_2 t^{\frac{1}{2}} \tag{5}$$

This model is one of the most commonly used to describe drug release from matrix devices (Paul, 2011).

Weibull (W) model:

$$M_t/M_\infty = 1 - exp(-at^b) \tag{6}$$

This model is useful for fitting the drug release from nanosystems (Corsaro et al., 2021).

In all the equations, M_∞ represents the total amount of drug injected into the system at time 0. M_t denotes the cumulative release at time t, while t represents the release time. The parameters a, and b are specific indices related to the system characteristics.

2.6. Mechanical behavior

The mechanical properties of fully swollen hydrogels were evaluated through unconfined compression testing using cylindrical specimens after equilibration in bi-distilled water. Each sample, defined by an initial cross-sectional area A_0 and height h_0, was positioned between the plates of a Thermo Scientific HAAKE MARS 40 (Thermo Scientific, Karlsruhe, Germany), and compressed at a constant rate of 5 μm s^{-1} at 25 °C. Data were analyzed using HAAKE RheoWin Job Manager software. A slight preload, which did not affect the modulus evaluation (Vanderhooft et al., 2009), was applied to ensure proper contact between the sample and the plate. During testing, the plates' normal force F_N and displacement Δh were recorded over time. Engineering stress σ and strain ε were calculated as $\sigma = F_N/A_0$ and $\varepsilon = \Delta h/h_0$, respectively. The compressive modulus E_c was determined from the linear region of the stress-strain curve. For accuracy, three measurements were performed on each sample type.

2.7. Antimicrobial assay

The antifungal activity of hydrogels was evaluated using the Kirby-Bauer disk diffusion method on three *Candida* strains: *Candida albicans* 10231, *Candida parapsilosis* 22019, and *Candida kruseii* (clinical isolate). Sabouraud agar plates were prepared and inoculated uniformly with each *Candida* strain, standardized to a 0.5 McFarland turbidity standard (approximately 1–2 × 10^6 CFU/mL) using sterile cotton swabs. Hydrogel, pre-formed as small disks (6 mm in diameter), was placed on the inoculated agar plates using sterile forceps, ensuring even spacing of at least 20 mm between disks. Control disks impregnated only with the hydrogel solvent were included to assess baseline activity, while disks

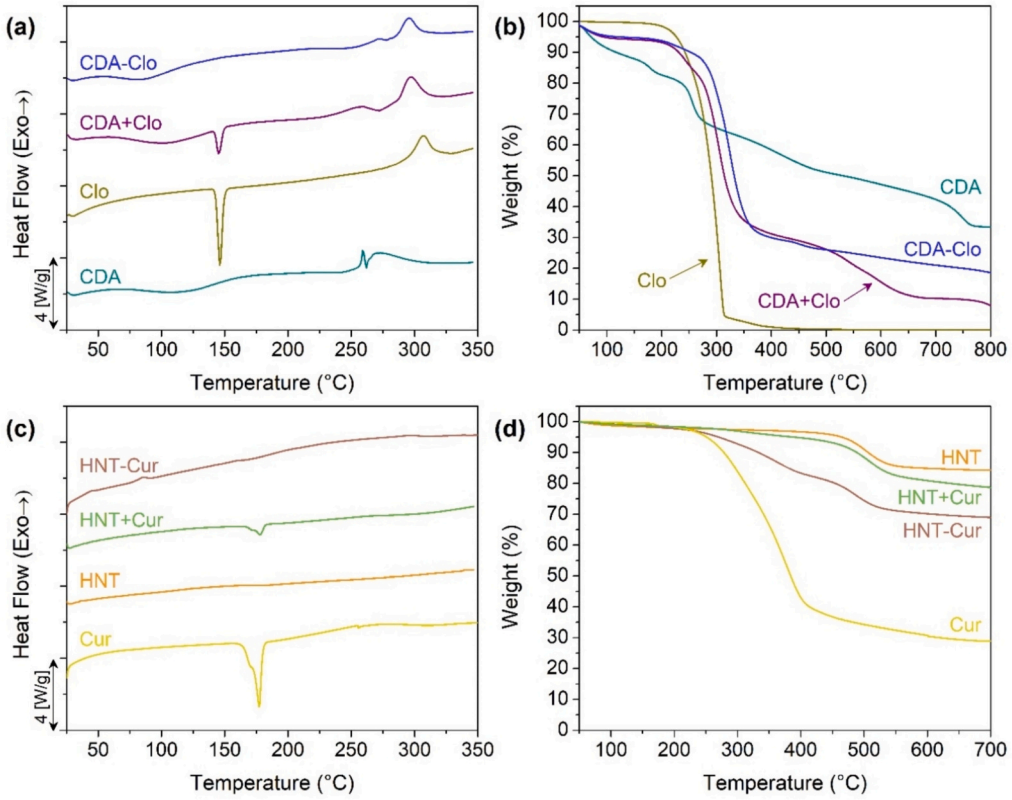

Fig. 2. DSC (a, c) and TGA (b, d) thermograms of the synthesized complexes (CDA-Clo and HNT-Cur), their respective starting compounds (Clo, CDA, HNT and Cur), and the physical mixtures (CDA + Clo and HNT + Cur).

containing Clo served as the positive control to validate antifungal efficacy. The plates were incubated at 33 °C for 24–48 h, after which the diameters of the inhibition zones were measured in millimeters to assess the hydrogel samples' antifungal efficacy.

2.8. Biocompatibility

H1HeLa CRL-1958™ cells were sourced from the American Type Culture Collection (Manassas, VA, USA). The cells were cultured in Leibovitz's L-15 medium supplemented with 2 mM L-glutamine, 10 % fetal bovine serum (FBS), and antibiotics (100 U/mL penicillin and 100 μg/mL streptomycin). Incubation was conducted in a humidified environment at 37 °C with a 5 % CO_2 atmosphere. Cell viability for the biocompatibility test was determined using the MTT assay, as per established protocols. In summary, 1.0×10^4 cells were seeded into 96-well plates and incubated for 24 h before treatment with H_CDA-Clo/HNT-Cur. Following treatment, MTT solution was added to each well, and the cells were incubated for 3 h. The resulting formazan crystals were dissolved in 150 μL of DMSO, and absorbance was recorded at 570 nm using a BioTek Synergy HTX microplate reader.

3. Results and discussion

3.1. Synthesis and characterization of CDA-Clo and HNT-Cur complexes

Inspired by literature showing that β-CD forms stable inclusion complexes with Clo (Ahmed et al., 1998; Mohammed et al., 2015), a similar approach has been adopted. However, to successfully incorporate cyclodextrin into the hydrogel matrix, it was necessary to modify β-CD to render it polymerizable *via* radical polymerization. Therefore, an acrylation reaction was performed to introduce polymerizable acrylate groups to β-CD, yielding the acrylated derivative (CDA) with a degree of acrylation around 3, as confirmed by ^{1}H NMR (Fig. S1). The acrylated derivative was then used to form an inclusion complex with Clo (Fig. 1).

The Clo incorporation into the hydrophobic cavity of CDA was achieved using a co-grinding method, in which equimolar amounts of the two components were ground together in a mortar for 20 min. Unlike other approaches, such as vacuum-assisted complexation, this method proved to be the most effective, yielding a stable complex (Jug & Mura, 2018). The success of the co-grinding approach was confirmed through thermal analyses (DSC and TGA), which demonstrated the effective integration of Clo into the cyclodextrin cavity. This two-step process, acrylation followed by complexation, enabled the incorporation of the Clo-loaded CDA into the hydrogel matrix, ensuring effective drug delivery and compatibility with the hydrogel structure.

Fig. 2 shows the thermal characterization (by TGA and DSC) of the complex obtained, along with the related starting compounds and physical mixture. As can be seen from the DSC trace (Fig. 2a), the physical mixture displays the characteristic signals of the starting products, while in the complex trace, as expected, the characteristic fusion signal of Clo (144 °C) disappears, confirming the successful formation of the complex (Taneri et al., 2004). Regarding the thermal analysis, the acrylated cyclodextrin exhibits an initial degradation starting around 140 °C, followed by a gradual and constant weight loss (Fig. 2b). The residue at 800 °C is approximately 37 %, likely due to structural distortion of the cyclodextrin ring caused by the insertion of the acrylic group in the molecule structure. This reaction promotes an increased formation of carbonaceous products, which remain stable at high temperatures, contributing to the higher residue at 800 °C. Clo exhibits evident degradation at 300 °C and no residue at 800 °C. The CDA-Clo complex shows a higher degradation temperature than the respective individual products and the related physical mixture, indicating a strong interaction between the molecules in the complex.

HNT was successfully loaded with Cur through a solution absorption method, a process designed to promote the efficient encapsulation of the

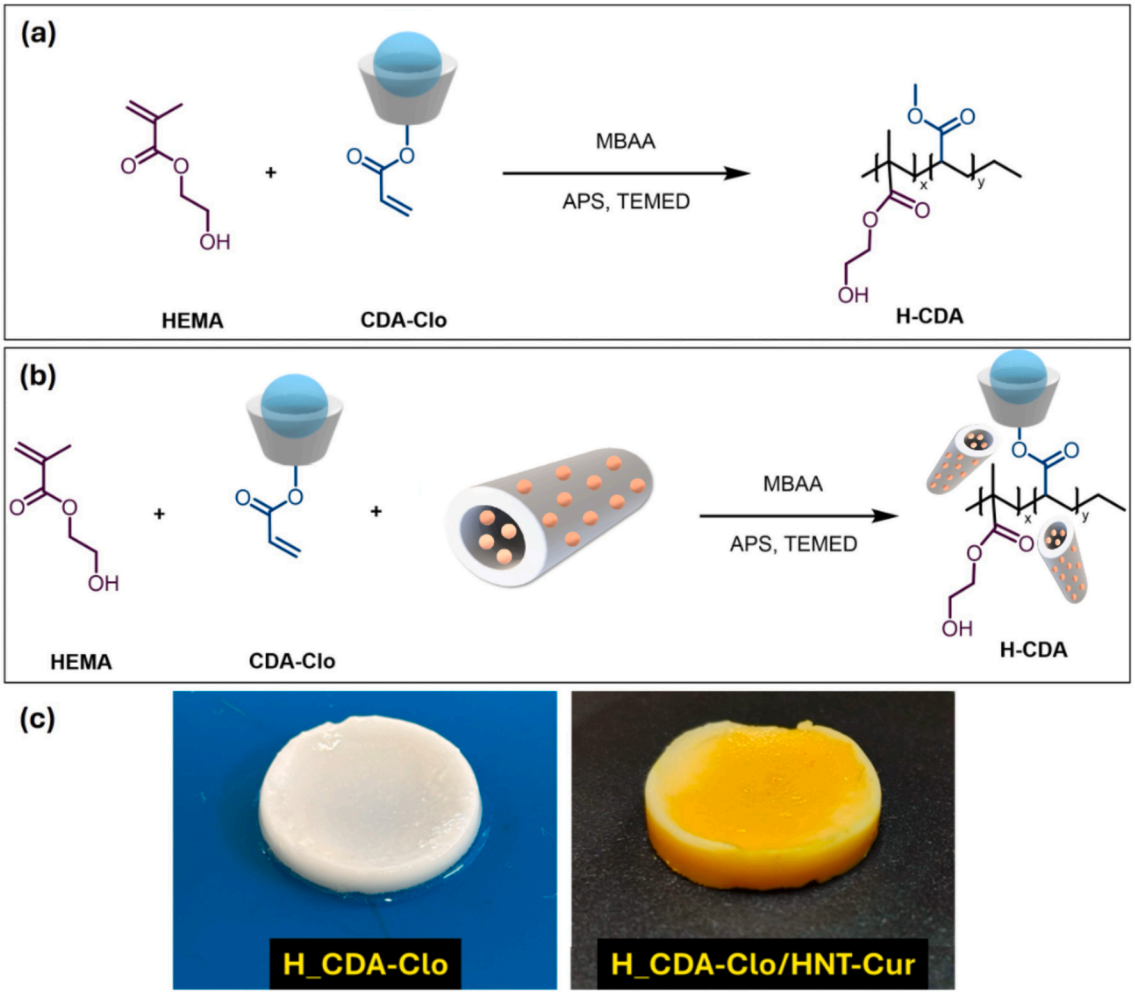

Fig. 3. (a,b) Synthesis of H_CDA-Clo and H_CDA-Clo/HNT-Cur hydrogels. (c) Photographic image of the two synthesized hydrogels.

compound within the inner lumen of the nanotubes, as confirmed by thermogravimetric analysis. TGA curves of Cur, HNT, HNT + Cur, and HNT-Cur are presented in Fig. 2d. The difference in residual weight between HNT and HNT-Cur reflects the contribution of Cur degradation, as it is thermally unstable and decomposes significantly during heating (Patamia et al., 2023).

The percentage of Cur in the HNT-Cur composite was determined by analyzing thermogravimetric data. The residual weight difference between HNT (84.14 %) and HNT-Cur (68.76 %) at 700 °C indicates a 15.38 % weight loss due to Cur degradation. Given that pure Cur shows a total weight loss of 71.0 %, the Cur content in HNT-Cur was calculated, following Eq. (7), as approximately 21.67 %.

$$\text{Cur content} = \frac{15.38}{71.0} \times 100 = 21.67\% \quad (7)$$

The thermal degradation profile of the HNT-Cur sample also shows increased thermal stability compared to pure Cur, indicating the protective effect of HNT on Cur against thermal decomposition. This confirms the successful incorporation of Cur into HNT, with improved thermal stability compared to pure Cur. Further confirmation of the formation of the complex was obtained through DSC analysis, as shown in Fig. 2c, similar to the CDA-Clo complex (Fig. 2a). The Cur fusion peak in the DSC trace of the complex disappeared while remaining visible in the trace of the physical mixture. The Cur-loaded nanotubes (HNT-Cur) were successful combined with a polymerizable mixture to be incorporated into the hydrogel system.

Table 1
The mass loss percentages of the synthesized hydrogels.

Sample	Mass loss [%]				
	T < 150 °C	150 °C < T < 350 °C	350 °C < T < 550 °C	550 °C < T < 800 °C	Residue
HNT	3.7	1.1	11.4	1.3	82.7
H_CDA	6.2	23.2	64.2	0.5	5.8
H_CDA/HNT	11.1	26.5	48.0	1.0	10.4
H_CDA/HNT-Cur	6.0	20.0	52.0	2.1	18.2
H_CDA-Clo	12.1	30.0	46.0	2.2	7.5
H_CDA-Clo/HNT	9.5	28.5	42.0	2.0	18.0
H_CDA-Clo/HNT-Cur	5.2	27.0	48.0	1.1	18.0

3.2. Synthesis and characterization of hydrogels

For the synthesis of hydrogels, HEMA co-monomer was mixed with CDA to improve the mechanical properties of the resulting material (Fig. 3). Pure CDA-based hydrogel, while effective for drug inclusion, is mechanically fragile and unsuitable for robust hydrogel formation. By incorporating HEMA, the hydrogel gains enhanced structural integrity and durability, overcoming the challenges of using 100 % CD alone. This combination ensures a more stable and resilient hydrogel system suitable for practical applications. A 1:1 weight ratio of CDA to HEMA was

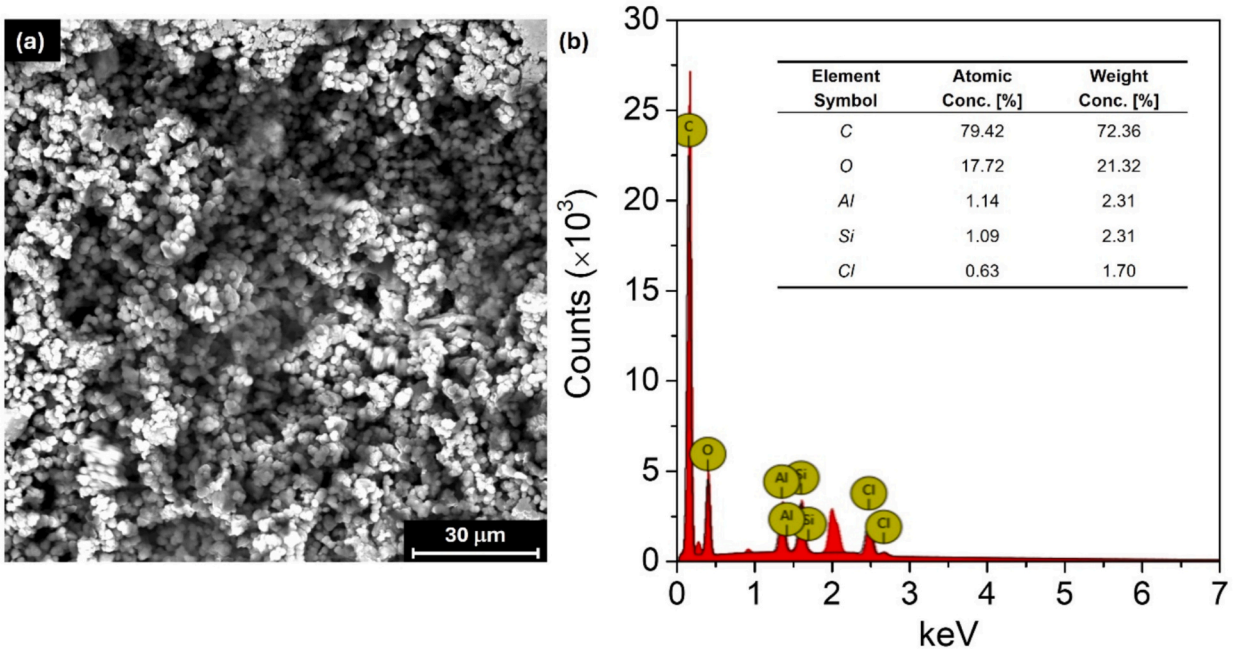

Fig. 4. (a) SEM and (b) EXD results of H_CD-Clo/HNT-Cur.

selected based on studies of hydrogel consistency, which identified this ratio as optimal for achieving both good mechanical strength and swelling capacity (Zagni et al., 2022). The co-polymerization of these monomers was carried out in the presence of MBAA at room temperature, using water as the solvent. The resulting hydrogel served as the blank control. To incorporate Clo into the material, the complex of acrylated cyclodextrin derivative containing the drug (CDA-Clo) was used as a monomer, forming the H_CDA-Clo hydrogel under identical polymerization conditions. For the Cur-loaded hydrogel, HNT-Cur was introduced to the polymerization mixture at a concentration of 20 % *w/w*, which did not adversely affect the polymerization process. This approach yielded the H_CDA-Clo/HNT-Cur hydrogel, a composite with increased drug delivery capacity.

The thermogravimetric analysis results, particularly the residue values at 800 °C (Table 1), reflect the percentage of HNT used for the hydrogel synthesis. The thermogram of H_CDA-Clo/HNT-Cur hydrogel is reported in the supporting information (Fig. S2).

The chemical structure of the synthesized copolymers was analyzed by FTIR spectroscopy. The signals are challenging to attribute due to the overlapping bands caused by the different components of the material. For example, the spectrum of H_CDA-Clo/HNT-Cur is shown in Fig. S3. The spectra present characteristic diagnostic bands at 1027 cm^{-1} (Cur) and 1073 cm^{-1} (HNT), assigned to the C—O stretch of phenyl alkyl and apical Si—O. Additionally, a broad transmittance peak at 3292 cm^{-1} is due to the valence vibrations of O—H bonds (C–OH).

Scanning Electron Microscopy (SEM) was utilized to investigate the morphology of the hydrogel samples. The SEM images reveal a microstructure characterized by a porous network interspersed with distinct spheroidal particulate features typical of hydrogels (Fig. 4a). This morphology is consistent with previous reports on similar materials based on HEMA monomer (Zagni, Coco, Dattilo, et al., 2023). As shown in higher magnification images, these particles exhibit sizes ranging from submicrometric dimensions to approximately 2 µm. The interconnected porous architecture indicates a typical hydrogel matrix, which is expected to support fluid retention and ion transport.

To verify the elemental composition and confirm the integration of all monomers within the hydrogel structure, Energy-Dispersive X-ray Spectroscopy (EDX) analysis was performed (Fig. 4b). The EDX spectra highlight the presence of key atoms consistent with the designed composition of the hydrogel. The distribution of these elements appears

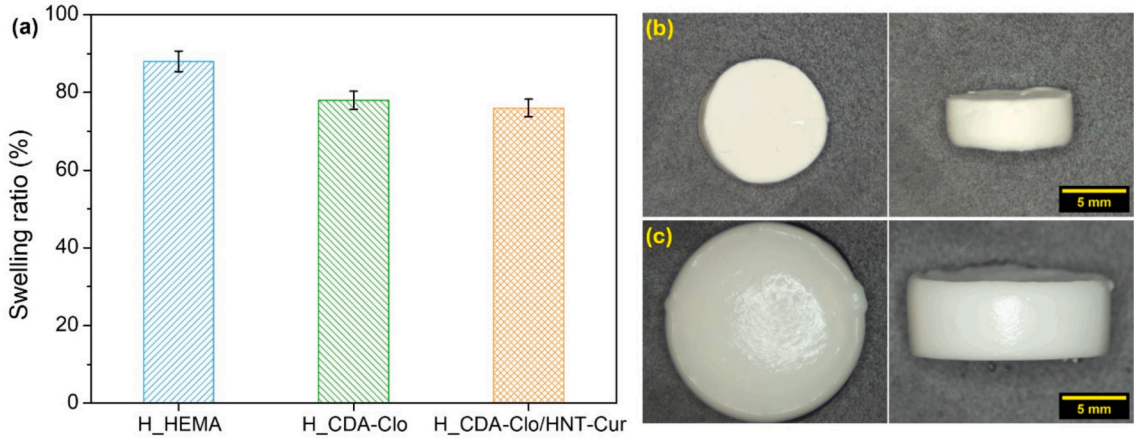

Fig. 5. (a) Swelling ratio of hydrogels; macroscopic images of H_HEMA samples before (dry state) (b) and after (c) swelling in water.

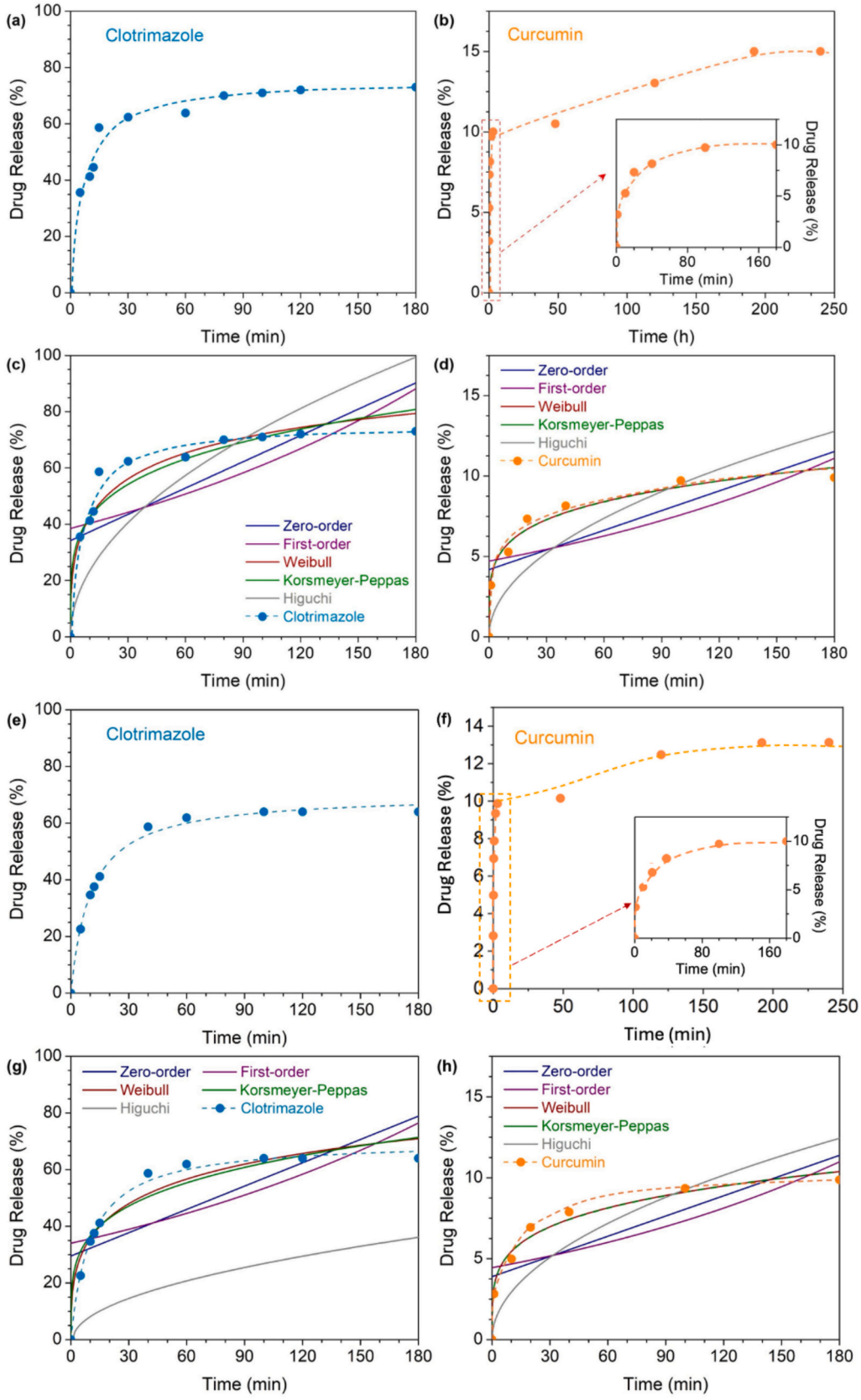

Fig. 6. Clo and Cur release (a,b) in neutral conditions and relative fitting curves (c,d); Clo and Cur release (e,f) in acidic environment and relative fitting curves (g,h).

uniform across the matrix and the embedded particles, suggesting successful incorporation or formation during the hydrogel synthesis process.

3.3. Swelling

The swelling behavior of the hydrogels highlights the influence of both the drug molecules and the structural components on water absorption capacity. The pure HEMA hydrogel exhibited the highest swelling ratio (88 %), as expected, due to its hydrophilic nature and absence of drug incorporation (Fig. 5a). The comparison of the volumetric change in H_HEMA, from its dry state (before swelling) to its swollen state (after water immersion), is shown in Fig. 5b and c. The incorporation of the Clo-loaded cyclodextrin complex (CDA-Clo) into the HEMA matrix resulted in a reduced swelling ratio (78 %), likely due to the hydrophobic nature of Clo and the steric hindrance introduced by the cyclodextrin cavities, which limit water uptake.

When CDA-Clo and Cur-loaded halloysite nanotubes (HNT-Cur) were embedded into the hydrogel (H_CDA-Clo/HNT-Cur), the swelling ratio decreased to 76 %. This reduction can be attributed to the combined effects of the hydrophobic Clo and the halloysite nanotubes, which occupy free spaces in the hydrogel network and restrict its expansion. Additionally, the structural confinement provided by HNT may further limit water penetration into the matrix.

Overall, the swelling ratio data demonstrate that drug incorporation and structural modifications, such as the addition of HNT, significantly impact the hydrogel's water absorption capacity. These results suggest that the designed hydrogels maintain sufficient swelling while achieving tailored drug-release properties.

3.4. Drug release

In vitro release experiments were conducted to evaluate the drug release capacity of the hydrogel system, and the results were analyzed using a previously constructed calibration curve for Clo and Cur through UV spectroscopy. The effective release of the drugs from their respective carriers was performed on CDA-Clo alone and HNT-Cur alone. The results showed that distinct rates and patterns characterize the two systems' drug release behaviors.

Including a free drug solution control for comparison in this study was not feasible due to inherent limitations in the hydrogel preparation process. The free drug introduced during the formulation was inevitably absorbed into the polymeric matrix, preventing the maintenance of a distinct free drug phase. Furthermore, the necessary washing steps to eliminate unreacted monomers and residual impurities also led to removing the unencapsulated drug, leaving only negligible traces. As a result, the establishment of meaningful free drug control was not only impractical but also scientifically uninformative for comparison purposes.

The release of Clo consisted of two main stages. Initially, there was a rapid release phase during the first 30 min (Fig. 6a), characterized by a release of approximately 62 %, likely due to the diffusion of the drug located near the surface of the polymer matrix or the CD cavities embedded within it. This burst release was followed by a slower, sustained release phase, with a release plateau of approximately 73 % achieved after 180 min. This biphasic pattern aligns with the diffusion of Clo from deeper within the polymer or the erosion of the matrix itself. The rapid initial release phase plays a crucial role in providing immediate antifungal activity and alleviating symptoms, while the sustained release over time helps maintain efficacy for controlling and ultimately curing the infection. Furthermore, the prolonged release profile of the antifungal agents in the formulation can significantly reduce the frequency of application compared to commercially available products, which typically require daily administration for three to seven days on average (Workowski & Bachmann, 2022).

In contrast, the release of Cur from the hydrogel exhibited a more gradual profile (Fig. 6b,c). The initial phase included a burst release of approximately 3.2 % in the first minute, attributed to the desorption of Cur weakly adsorbed on the nanotube surfaces. However, the release equilibrium was reached much more slowly, with 10.5 % released after 48 h and a final plateau of approximately 15 % after 8 days (Riela et al., 2014). This sustained release reflects the structural confinement provided by the nanotubes and the slower diffusion of Cur through the hydrogel matrix, governed by Fickian diffusion and possible interactions with the inner surfaces of the HNT.

Analysis of the empirical data, fitted using the equations described in the Experimental section, identified two top-performing models. The Weibull model provided the best fit, with R^2 values of 0.95 and 0.98 for Clo and Cur release, respectively. The Korsmeyer–Peppas model followed closely, showing R^2 values of 0.92 and 0.98 for Clo and Cur release, respectively. Weibull and Korsmeyer-Peppas models provided both excellent fit for the experimental data. For Clo, the release exponent value ($n = 0.22$) from the Korsmeyer-Peppas model suggests a Fickian diffusion mechanism consistent with the initial rapid diffusion facilitated by the CD's cavities. On the other hand, the n-value for Cur ($n = 0.2$) indicated a more complex mechanism involving both Fickian diffusion and interactions with the HNT surfaces, contributing to its extended release profile.

The Weibull model reinforced these observations. Clo's rapid release was reflected in a steeper initial slope (higher n), while Cur exhibited a more gradual curve, indicative of its slower and more sustained diffusion. The time-related constant (k) was also lower for Cur, emphasizing the slower release rate compared to Clo.

These findings highlight the distinct release dynamics of the two drug-carrier systems embedded within the hydrogel. Clo's rapid release from cyclodextrin cavities makes it ideal for applications requiring immediate therapeutic action, while Cur's prolonged release due to the structural properties of HNT supports sustained therapeutic effects over an extended period. This dual-release profile showcases the hydrogel's potential to provide tailored release kinetics, optimizing efficacy in multi-drug delivery applications.

The release profiles of Clo and Cur under acidic conditions did not show significant changes compared to the neutral pH, although the overall release was lower. This behavior is illustrated in Fig. 6e,f, which display the release profiles of Clo and Cur, respectively, in acidic conditions. The fitting parameters, shown in Fig. 6g,h, are comparable to those observed at neutral pH, indicating that the release mechanisms remain consistent despite the pH variation.

3.5. Antifungal activity

The hydrogel system was strategically designed to incorporate an optimal amount of Clo and Cur to achieve the desired antifungal, antioxidant, and anti-inflammatory effects. Curcumin, in addition to its well-documented anti-inflammatory properties, also exhibits potent antifungal activity, making it a valuable synergistic partner to clotrimazole. Considering the distinct role of each molecule within the system, a Clo/Cur (w/w) ratio of 2.5:1 was selected, corresponding to approximately 850 μg of Clo and 340 μg of Cur per disk. These values were determined through a theoretical calculation based on the initial quantities and polymerization yield. This ratio corresponds to a molar ratio of approximately 2.67:1, ensuring an optimal balance between the distinct roles of each compound in delivering antifungal, antioxidant, and anti-inflammatory effects. This carefully optimized composition ensures robust antifungal efficacy by leveraging curcumin's synergistic potential while adhering to safe dosage limits. Notably, Cur has been shown to exert significant antifungal activity, with a concentration of 200 μg/mL demonstrated to create an inhibition zone against fungal growth (Sharma et al., 2010), further supporting its role in enhancing the overall effectiveness of the hydrogel system.

The antifungal activity of the hydrogels was tested against *C. krusei*, *C. albicans* 10231, and *C. parapsilosis* 22019, highlighting the role of Clo

Table 2
Antifungal activity of hydrogel formulations against *C. krusei*, *C. albicans* 10231, and *C. parapsilosis* 22019, expressed as inhibition zone diameters (mm).

Name	*C. krusei*	*C. albicans* 10231	*C. parapsilosis* 22019
H_CDA/HNT-Cur	10.1 ± 0.1	10.3 ± 0.2	10.2 ± 0.1
H_CDA/HNT (Blank)	NA	NA	NA
H_CDA-Clo	32.2 ± 0.1	24.2 ± 0.3	36.3 ± 0.1
Clo10 (internal positive control)	33.2 ± 0.1	22.1 ± 0.2	33.1 ± 0.3
H_CDA-Clo/HNT-Cur	39.2 ± 0.2	39.1 ± 0.2	42.1 ± 0.2

and Cur in enhancing fungal inhibition (Table 2). The blank hydrogel (Disk 4), composed of cyclodextrin and halloysite nanotubes, showed no antifungal activity, serving as a negative control (Fig. 7). The hydrogel loaded only with Clo (Disk 5) exhibited inhibition zones comparable to the Clo-positive control (Disk 7), with zones of 32.2 ± 0.1 mm, 24.2 ± 0.3 mm, and 36.3 ± 0.1 mm for *C. krusei*, *C. albicans* 10231, and *C. parapsilosis* 22019, respectively, confirming that the hydrogel matrix does not interfere with Clo's activity. The hydrogel loaded solely with Cur (Disk 1) showed moderate antifungal effects with inhibition zones of 10 mm across all strains, indicating lower potency than Clo. The Clo-positive control (Disk 7) produced inhibition zones of 33.2 ± 0.1 mm, 22.1 ± 0.2 mm, and 33.1 ± 0.3 mm, validating the assay and Clo's efficacy. Finally, the dual-loaded hydrogel (Disk 9), containing both Clo and Cur, demonstrated the highest antimycotic activity with zones of 39.2 ± 0.2 mm, 39.1 ± 0.2 mm, and 42.1 ± 0.2 mm against *C. krusei*, *C. albicans* 10231, and *C. parapsilosis* 22019, respectively. This enhanced activity suggests a synergistic or additive effect between Clo and Cur, emphasizing the potential of the dual-loaded hydrogel as an advanced antifungal material with optimized release properties.

The results highlight the promise of the dual-loaded hydrogel (H_CDA-Clo/HNT-Cur) as an advanced antifungal material. The enhanced activity likely stems from the synergistic antifungal effects of Clo and Cur, coupled with the controlled and sustained release profile enabled by the hydrogel matrix. These findings underscore the effectiveness of integrating multiple active compounds within a unified hydrogel system to achieve superior antifungal performance.

3.6. Biocompatibility

The biocompatibility of the dual-loaded hydrogel H_CDA-Clo/HNT-Cur, containing both Clo and Cur, was assessed on vaginal epithelial cells using H1HeLa CRL-1958 cells as a representative model. Testing on HeLa cells was critical due to their relevance as a human-derived epithelial cell line, which provides insights into the material's potential application in sensitive biological environments. Cell viability was evaluated through the MTT assay, wherein the hydrogel demonstrated no significant cytotoxicity, as shown in Fig. 8. The hydrogel maintained the cell viability above acceptable thresholds, indicating its safety and biocompatibility for epithelial tissues. This result underscores the importance of the hydrogel's compatibility for applications in vaginal antifungal treatments, where maintaining the health of epithelial cells is essential for therapeutic efficacy and user safety. The use of HeLa cells further validated the suitability of this hydrogel for human use, reinforcing its capability as a biocompatible and effective delivery system for dual antifungal and anti-inflammatory agents.

3.7. Mechanical behavior

The mechanical properties of hydrogels are critical for their suitability in biomedical applications, where appropriate mechanical resistance is essential to ensure reliable performance under physiological conditions. Unconfined uniaxial compression tests were conducted to assess these properties. The stress-strain curves of the samples, measured under fully water-saturated conditions, are presented in Fig. 9a. HEMA-based hydrogels demonstrated a consistent stress-strain response, characterized by an initial linear elastic region extending up

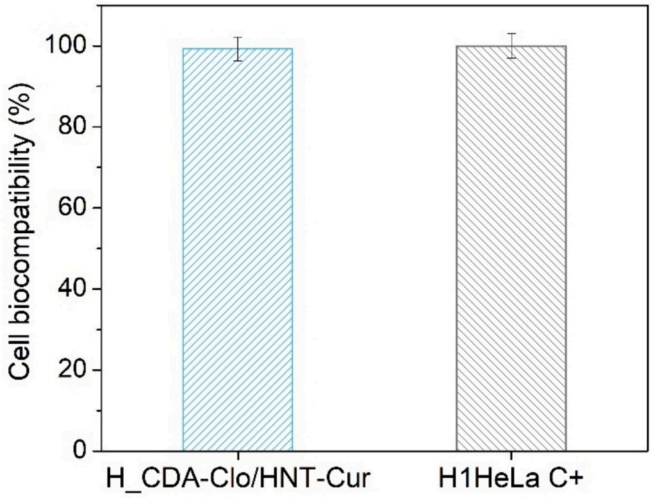

Fig. 8. Cell viability assessment of H1HeLa cells treated with the dual-loaded cryogel H_CDA-Clo/HNT-Cur.

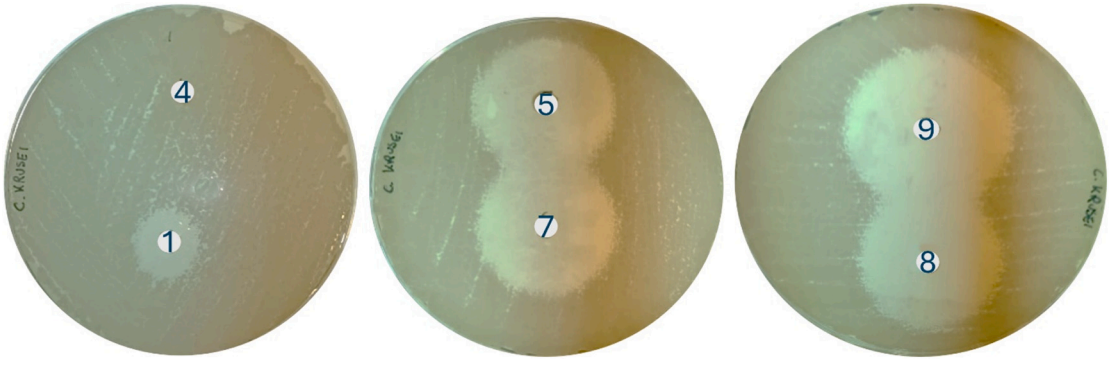

Fig. 7. Kirby-Bauer test results showing the antifungal activity of hydrogel formulations against *Candida krusei*. The image displays inhibition zones corresponding to the tested formulations: Disk 1 (H_CDA/HNT-Cur), Disk 4 (H_CDA/HNT, Blank), Disk 5 (H_CDA-Clo), Disk 7 (Clo 10, positive control with Clo at 10 mg), Disk 8 (Clo 20, positive control with Clo at 20 mg), and Disk 9 (H_CDA-Clo/HNT-Cur). Clear zones of inhibition indicate the antifungal efficacy of each formulation, with the positive controls (Disks 7 and 8) serving as references for comparison.

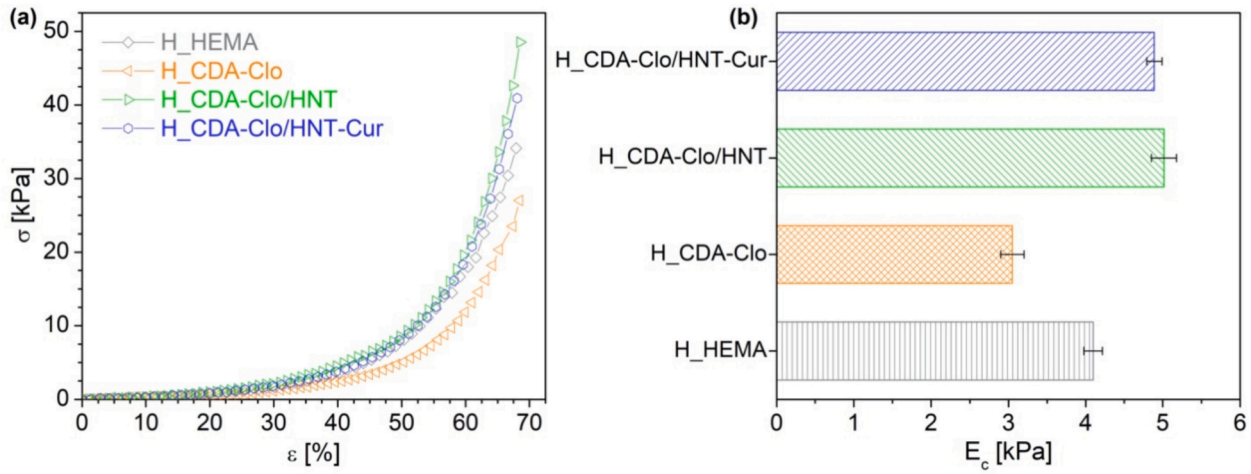

Fig. 9. Compression stress-strain curve (a) and average compressive modulus (b) of the hydrogels.

to 25 % strain, followed by an exponential increase in stress. The extrapolated values of the elastic-linear modulus reveal that the incorporation of β-cyclodextrin reduces the compressive modulus (E_c) by 25 %, likely due to changes in the network structure or interactions that decrease the material flexibility (Fig. 9b). However, this reduction in stiffness is effectively counteracted by adding 20 % halloysite which enhances the compressive modulus by approximately 25 % compared to the pure HEMA hydrogel. This recovery and enhancement of mechanical properties suggest a synergistic interaction between the matrix and halloysite, improving material performance. This mechanical behavior highlights the material's ability to maintain structural integrity under moderate strain while providing enhanced resistance to deformation at higher strain levels. Such properties are critical for ensuring durability and functionality in biomedical environments, where materials must withstand dynamic mechanical stresses without compromising performance.

4. Conclusions

The integration of advanced materials and technologies into vaginal drug delivery systems is setting the stage for more effective therapies in women's health, ultimately improving the overall efficacy of treatments and patient quality of life. In this context, a novel drug delivery system composed of natural and biocompatible materials was developed to address the limitations of conventional treatments for vaginal infections.

The integration of cyclodextrins and halloysite nanotubes into a single system offers a synergistic approach to vaginal drug delivery. Clo, encapsulated within cyclodextrins, is released at a relatively fast yet consistent rate, ensuring rapid onset of antifungal action while maintaining therapeutic levels. Simultaneously, the gradual release mechanism afforded by HNT ensures prolonged therapeutic effects, reduces dosing frequency, and enhances patient compliance. Additionally, HNT contribute to improving the mechanical properties of the hydrogel, enhancing its structural stability and usability during application. This innovative strategy holds significant potential for improving the efficacy, convenience, and durability of treatments for vaginal infections while minimizing side effects.

This dual-release system ensures a high local concentration of both therapeutic agents over time, likely enhancing the efficacy of infection treatment while minimizing systemic side effects and reducing the risk of antibiotic resistance.

CRediT authorship contribution statement

Elisabetta Grazia Tomarchio: Writing – original draft, Visualization, Investigation, Formal analysis. **Chiara Zagni:** Writing – original draft, Visualization, Validation, Supervision, Methodology, Conceptualization. **Sandro Dattilo:** Writing – original draft, Methodology, Investigation, Formal analysis. **Libera Vitiello:** Writing – original draft, Methodology, Investigation, Formal analysis. **Virginia Fuochi:** Writing – original draft, Supervision, Investigation, Data curation. **Salvatore Furnari:** Methodology, Formal analysis. **Pio Maria Furneri:** Writing – review & editing, Supervision. **Giuseppe Granata:** Writing – review & editing, Methodology, Investigation. **Sabrina Carola Carroccio:** Writing – review & editing, Resources, Funding acquisition. **Antonio Rescifina:** Writing – review & editing, Validation, Project administration.

Funding

This research was partially funded by the European Union (Next-Generation EU) through the MIUR-PNRR project SAMOTHRACE-Sicilian MicronanoTech Research and Innovation Center (ECS00000022, CUP B63C22000620005).

Declaration of competing interest

The authors declare that they have no known competing financial interests or personal relationships that could have appeared to influence the work reported in this paper.

Appendix A. Supplementary data

Supplementary data to this article can be found online at https://doi.org/10.1016/j.carbpol.2025.123412.

Data availability

No data was used for the research described in the article.

References

Ahmed, M. O., El-Gibaly, I., & Ahmed, S. M. (1998). Effect of cyclodextrins on the physicochemical properties and antimycotic activity of clotrimazole. *International Journal of Pharmaceutics, 171*, 111–121. https://doi.org/10.1016/S0378-5173(98)00163-X

Andrade, J. T., Fantini de Figueiredo, G., Cruz, L. F., Eliza de Morais, S., Souza, C. D. F., Pinto, F. C. H., … de F. Araújo, M. G. (2019). Efficacy of curcumin in the treatment of experimental vulvovaginal candidiasis. *Revista Iberoamericana de Micología, 36*, 192–199. https://doi.org/10.1016/j.riam.2019.01.003

Carbone, C., Fuochi, V., Zielińska, A., Musumeci, T., Souto, E. B., Bonaccorso, A., … Furneri, P. M. (2020). Dual-drugs delivery in solid lipid nanoparticles for the

treatment of Candida albicans mycosis. *Colloids and Surfaces. B, Biointerfaces, 186*, Article 110705. https://doi.org/10.1016/j.colsurfb.2019.110705

Chen, N., Deng, J., Zhang, Z., Feng, X., Wang, H., Chen, J., Li, L., Cao, Y., Jia, C., & Cao, Y. (2022). Oxidative stress-triggered pyroptosis mediates *Candida albicans* susceptibility in diabetic foot. *Microbial Pathogenesis, 172*, Article 105765. https://doi.org/10.1016/j.micpath.2022.105765

Cheng, K. O., Montaño, D. E., Zelante, T., Dietschmann, A., & Gresnigt, M. S. (2024). Inflammatory cytokine signalling in vulvovaginal candidiasis: A hot mess driving immunopathology. *Oxford Open Immunology, 5*, Article iqae010. https://doi.org/10.1093/oxfimm/iqae010

Corsaro, C., Neri, G., Mezzasalma, A. M., & Fazio, E. (2021). Weibull modeling of controlled drug release from ag-PMA nanosystems. *Polymers, 13*, 2897. https://doi.org/10.3390/polym13172897

Crowley, P. D., & Gallagher, H. C. (2014). Clotrimazole as a pharmaceutical: Past, present and future. *Journal of Applied Microbiology, 117*, 611–617. https://doi.org/10.1111/jam.12554

d'Enfert, C., Kaune, A.-K., Alaban, L.-R., Chakraborty, S., Cole, N., Delavy, M., … Brown, A. J. P. (2020). The impact of the Fungus-Host-Microbiota interplay upon Candida albicans infections: Current knowledge and new perspectives. *FEMS Microbiology Reviews, 45*, Article fuaa060. https://doi.org/10.1093/femsre/fuaa060

Dreiss, C. A. (2020). Hydrogel design strategies for drug delivery. *Current Opinion in Colloid & Interface Science, 48*, 1–17. https://doi.org/10.1016/j.cocis.2020.02.001

Ezike, T. C., Okpala, U. S., Onoja, U. L., Nwike, C. P., Ezeako, E. C., Okpara, O. J., Okoroafor, C. C., Eze, S. C., Kalu, O. L., Odoh, E. C., Nwadike, U. G., Ogbodo, J. O., Umeh, B. U., Ossai, E. C., & Nwanguma, B. C. (2023a). Advances in drug delivery systems, challenges and future directions. *Heliyon, 9*, Article e17488. https://doi.org/10.1016/j.heliyon.2023.e17488

Ezike, T. C., Okpala, U. S., Onoja, U. L., Nwike, C. P., Ezeako, E. C., Okpara, O. J., Okoroafor, C. C., Eze, S. C., Kalu, O. L., Odoh, E. C., Nwadike, U. G., Ogbodo, J. O., Umeh, B. U., Ossai, E. C., & Nwanguma, B. C. (2023b). Advances in drug delivery systems, challenges and future directions. *Heliyon, 9*, Article e17488. https://doi.org/10.1016/j.heliyon.2023.e17488

Fuochi, V., Li Volti, G., & Furneri, P. M. (2017). Commentary: Lactobacilli dominance and vaginal pH: Why is the human vaginal microbiome unique? *Frontiers in Microbiology, 8*. https://doi.org/10.3389/fmicb.2017.01815

Furneri, P. M., Petronio, G. P., Fuochi, V., Cupri, S., & Pignatello, R. (2017). Chapter 23 - Nanosized devices as antibiotics and antifungals delivery: Past, news, and outlook. In E. Andronescu, & A. M. Grumezescu (Eds.), *Nanostructures for drug delivery* (pp. 697–748). Elsevier. https://doi.org/10.1016/B978-0-323-46143-6.00023-3.

Garcia-Gomes, A. S., Curvelo, J. A. R., Soares, R. M. A., & Ferreira-Pereira, A. (2012). Curcumin acts synergistically with fluconazole to sensitize a clinical isolate of Candida albicans showing a MDR phenotype. *Medical Mycology, 50*, 26–32. https://doi.org/10.3109/13693786.2011.578156

Jablan, J., Bačić, I., Kujundžić, N., & Jug, M. (2013). Zaleplon co-ground complexes with natural and polymeric β-cyclodextrin. *Journal of Inclusion Phenomena and Macrocyclic Chemistry, 76*, 353–362. https://doi.org/10.1007/s10847-012-0206-9

Jug, M., & Mura, P. A. (2018). Grinding as solvent-free green chemistry approach for cyclodextrin inclusion complex preparation in the solid state. *Pharmaceutics, 10*, 189. https://doi.org/10.3390/pharmaceutics10040189

Karaman, M., Arıkan Ayyıldız, Z., Fırıncı, F., Kiray, M., Bağrıyanık, A., Yilmaz, O., … Karaman, Ö. (2011). Effects of curcumin on lung histopathology and fungal burden in a mouse model of chronic asthma and oropharyngeal candidiasis. *Archives of Medical Research, 42*, 79–87. https://doi.org/10.1016/j.arcmed.2011.01.011

Lee, W., & Lee, D. G. (2014). An antifungal mechanism of curcumin lies in membrane-targeted action within andida albicans. *IUBMB Life, 66*, 780–785. https://doi.org/10.1002/iub.1326

Li, L., Fan, H., Wang, L., & Jin, Z. (2016). Does halloysite behave like an inert carrier for doxorubicin? *RSC Advances, 6*, 54193–54201. https://doi.org/10.1039/C6RA09198A

Lin, L., & Lee, K.-H. (2006). Structure-activity relationships of curcumin and its analogs with different biological activities†. In Atta-ur-Rahman (Ed.), *Studies in natural products chemistry* (pp. 785–812). Elsevier. https://doi.org/10.1016/S1572-5995(06)80040-2.

Mahant, S., Sharma, A. K., Gandhi, H., Wadhwa, R., Dua, K., & Kapoor, D. N. (2023). Emerging trends and potential prospects in vaginal drug delivery. *Current Drug Delivery, 20*, 730–751. https://doi.org/10.2174/1567201819666220413131243

Martínez-Pérez, B., Quintanar-Guerrero, D., Tapia-Tapia, M., Cisneros-Tamayo, R., Zambrano-Zaragoza, M. L., Alcalá-Alcalá, S., Mendoza-Muñoz, N., & Piñón-Segundo, E. (2018). Controlled-release biodegradable nanoparticles: From preparation to vaginal applications. *European Journal of Pharmaceutical Sciences, 115*, 185–195. https://doi.org/10.1016/j.ejps.2017.11.029

Mohammed, N. N., Pandey, P., Khan, N. S., Elokely, K. M., Liu, H., Doerksen, R. J., & Repka, M. A. (2015). Clotrimazole-cyclodextrin based approach for the management and treatment of Candidiasis - A formulation and chemistry based evaluation. *Pharmaceutical Development and Technology, 21*, 619. https://doi.org/10.3109/10837450.2015.1041041

Mohammed, N. N., Pandey, P., Khan, N. S., Elokely, K. M., Liu, H., Doerksen, R. J., & Repka, M. A. (2016). Clotrimazole-cyclodextrin based approach for the management and treatment of Candidiasis - A formulation and chemistry based evaluation. *Pharmaceutical Development and Technology, 21*, 619–629. https://doi.org/10.3109/10837450.2015.1041041

Mulye, N. V., & Turco, S. J. (1995). A simple model based on first order kinetics to explain release of highly water soluble drugs from porous dicalcium phosphate dihydrate matrices. *Drug Development and Industrial Pharmacy*. https://doi.org/10.3109/03639049509026658

Nicolau Costa, K. M., Sato, M. R., Barbosa, T. L. A., Rodrigues, M. G. F., Medeiros, A. C. D., de L. Damasceno, B. P. G., & Oshiro-Júnior, J. A. (2021). Curcumin-loaded micelles dispersed in ureasil-polyether materials for a novel sustained-release formulation. *Pharmaceutics, 13*, 675. https://doi.org/10.3390/pharmaceutics13050675

Patamia, V., Zagni, C., Fiorenza, R., Fuochi, V., Dattilo, S., Riccobene, P. M., … Rescifina, A. (2023). Total bio-based material for drug delivery and iron chelation to fight cancer through antimicrobial activity. *Nanomaterials, 13*, 2036. https://doi.org/10.3390/nano13142036

Paul, D. R. (2011). Elaborations on the Higuchi model for drug delivery. *International Journal of Pharmaceutics, 418*, 13–17. https://doi.org/10.1016/j.ijpharm.2010.10.037

Pedersen, M. (1993). Effect of hydrotropic substances on the complexation of clotrimazole with β-cyclodextrin. *Drug Development and Industrial Pharmacy, 19*, 439–448. https://doi.org/10.3109/03639049309063201

Peng, L., Liu, S., Feng, A., & Yuan, J. (2017). Polymeric nanocarriers based on cyclodextrins for drug delivery: Host–guest interaction as stimuli responsive linker. *Molecular Pharmaceutics, 14*, 2475–2486. https://doi.org/10.1021/acs.molpharmaceut.7b00160

Peppas, N. A. (1985). Analysis of Fickian and non-Fickian drug release from polymers. *Pharmaceutica Acta Helvetiae, 60*(4), 110–111. PMID: 4011621.

Raina, N., Pahwa, R., Bhattacharya, J., Paul, A. K., Nissapatorn, V., de L. Pereira, M., … Gupta, M. (2022). Drug delivery strategies and biomedical significance of hydrogels: Translational considerations. *Pharmaceutics, 14*, 574. https://doi.org/10.3390/pharmaceutics14030574

Reef, S. E., Levine, W. C., McNeil, M. M., Fisher-Hoch, S., Holmberg, S. D., Duerr, A., … Pinner, R. W. (1993). Treatment options for vulvovaginal candidiasis. *Clinical Infectious Diseases, 20*(1995), S80–S90. https://doi.org/10.1093/clinids/20.Supplement_1.S80

Riela, S., Massaro, M., Colletti, C. G., Bommarito, A., Giordano, C., Milioto, S., Noto, R., Poma, P., & Lazzara, G. (2014). Development and characterization of co-loaded curcumin/triazole-halloysite systems and evaluation of their potential anticancer activity. *International Journal of Pharmaceutics, 475*, 613–623. https://doi.org/10.1016/j.ijpharm.2014.09.019

Sharma, M., Manoharlal, R., Negi, A. S., & Prasad, R. (2010). Synergistic anticandidal activity of pure polyphenol curcumin I in combination with azoles and polyenes generates reactive oxygen species leading to apoptosis. *FEMS Yeast Research, 10*, 570–578. https://doi.org/10.1111/j.1567-1364.2010.00637.x

Siepmann, J., & Siepmann, F. (2013). Mathematical modeling of drug dissolution. *International Journal of Pharmaceutics, 453*, 12–24. https://doi.org/10.1016/j.ijpharm.2013.04.044

Taneri, F., Güneri, T., Aigner, Z., Berkesi, O., & Kata, M. (2004). Thermoanalytical studies on complexes of clotrimazole with cyclodextrins. *Journal of Thermal Analysis and Calorimetry, 76*, 471–479. https://doi.org/10.1023/B:JTAN.0000028026.30886.ae

Vanderhooft, J. L., Alcoutlabi, M., Magda, J. J., & Prestwich, G. D. (2009). Rheological properties of cross-linked hyaluronan-gelatin hydrogels for tissue engineering. *Macromolecular Bioscience, 9*, 20–28. https://doi.org/10.1002/mabi.200800141

Varaprasad, K., Raghavendra, G. M., Jayaramudu, T., Yallapu, M. M., & Sadiku, R. (2017). A mini review on hydrogels classification and recent developments in miscellaneous applications. *Materials Science and Engineering: C, 79*, 958–971. https://doi.org/10.1016/j.msec.2017.05.096

Vergaro, V., Abdullayev, E., Lvov, Y. M., Zeitoun, A., Cingolani, R., Rinaldi, R., & Leporatti, S. (2010). Cytocompatibility and uptake of halloysite clay nanotubes. *Biomacromolecules, 11*, 820–826. https://doi.org/10.1021/bm9014446

Witika, B. A., Makoni, P. A., Matafwali, S. K., Mweetwa, L. L., Shandele, G. C., & Walker, R. B. (2021). Enhancement of biological and pharmacological properties of an encapsulated polyphenol: Curcumin. *Molecules, 26*, 4244. https://doi.org/10.3390/molecules26144244

Workowski, K. A., & Bachmann, L. H. (2022). Centers for Disease Control and Prevention's sexually transmitted diseases infection guidelines. *Clinical Infectious Diseases, 74*, S89–S94. https://doi.org/10.1093/cid/ciab1055

Zagni, C., Coco, A., Dattilo, S., Patamia, V., Floresta, G., Fiorenza, R., Curcuruto, G., Mecca, T., & Rescifina, A. (2023). HEMA-based macro and microporous materials for CO2 capture. *Materials Today Chemistry, 33*, Article 101715. https://doi.org/10.1016/j.mtchem.2023.101715

Zagni, C., Coco, A., Mecca, T., Curcuruto, G., Patamia, V., Mangano, K., … Carroccio, S. C. (2023). Sponge-like macroporous cyclodextrin-based cryogels for controlled drug delivery. *Materials Chemistry Frontiers, 7*, 2693–2705. https://doi.org/10.1039/D3QM00139C

Zagni, C., Dattilo, S., Mecca, T., Gugliuzzo, C., Scamporrino, A. A., Privitera, V., Puglisi, R., & Carola Carroccio, S. (2022). Single and dual polymeric sponges for emerging pollutants removal. *European Polymer Journal, 179*, Article 111556. https://doi.org/10.1016/j.eurpolymj.2022.111556

Zagni, C., Patamia, V., Dattilo, S., Fuochi, V., Furnari, S., Furneri, P. M., … Rescifina, A. (2024). Supramolecular biomaterials as drug nanocontainers with iron depletion properties for antimicrobial applications. *Materials Advances, 5*, 3675–3682. https://doi.org/10.1039/D3MA00918A

Zagni, C., Scamporrino, A. A., Riccobene, P. M., Floresta, G., Patamia, V., Rescifina, A., & Carroccio, S. C. (2023). Portable nanocomposite system for wound healing in space. *Nanomaterials, 13*, 741. https://doi.org/10.3390/nano13040741